Plk5, a Polo-box domain-only protein with specific roles in neuron differentiation and glioblastoma suppression

By Guillermo de Cárcer *et al*.

Supplementary Figures

Figure S1. Sequence analysis of Plk5 in mammals. A. The murine Plk5 protein is most similar to Plk2 and Plk3 both in mice and humans. The structure of the kinase domain and the polo-box domain (PBD) is shown as well as critical residues in these domains. The tree was calculated using the average distance method BLOSUM62 (1). A similar tree is obtained when comparing only the kinase domain (data not shown). B. *Plk5* gene structure in the mouse and human genomes. Coding exons are shown as grey boxes whereas non-coding exons are empty boxes. Filled boxes indicate the kinase domain at the N-terminus of the protein and the PBDs at the C-terminus. C, Primary sequence of mouse Plk proteins at the ATP binding pocket and the activation loop of the kinase domain. Two relevant changes in Plk5 are shown in red boxes. The DFG motif is altered in the new Plk5 member. The activation threonine located at the T-loop is missing in the Plk5 sequence. D, Sequence comparison of the two PBDs in the murine Plk1, Plk2, Plk3 and Plk5 proteins. The critical tryptophan (W in the red box) in PBD1 is maintained in Plk5. However, two critical residues (H and K in the red boxes) involved in phospho-target recognition in PBD2 are not conserved in this new family member.

Figure S2. Analysis of the stop codon in exon 6 of human *PLK5*. Human DNA blood samples extracted from healthy individuals and DNA from HeLa, PC3 and U2OS cells were amplified by

nested PCR using two different pair of oligonucleotides (red and green arrows). The final expected fragments of 230 bp were sequenced and the stop codon was confirmed in all these samples.

Figure S3. Comparison of cell cycle defects and induction of apoptosis by the PBD of Plk family members. NIH3T3 cells were transfected with the human PLK1, PLK2 and PLK3 PBD domains fused to EGFP, or with the human PLK5 cDNA. Upon 24 hours expression, cells were fixed and analysed for cell cycle profile at the FACs. hPLK5 leads to a significant reduction of cells in S and G2/M phases. PLK1-PBD and PLK3-PBD do not significantly change the cell cycle profile and PLK2-PBD leads to partial arrest in G1. B, Similar overexpression experiments were performed in two GBM cell lines (U87 and U373) in order to analyze the induction of apoptosis, as measured by the ratio of Annexin V-positive cells.

Figure S4. Analysis of antibodies against the mouse Plk5 protein. Two different peptides at the N-terminus (NT) and the linker (LK) region were used and two different sera SG3509 and SG3510 for NT, and SG3511 and SG3512 for LK were tested for each position. Human HEK293 cells were transfected with GFP (lanes 1), GFP-Plk1 (lanes 2) and two independent transfections with GFP-Plk5 (lanes 3 and 4). The immunodetection with GFP antibodies detect both GFP-Plk1 and GFP-Plk5 constructs (red arrows). The Plk5-NT antibody SG3509 (4^{th} bleed) efficiently detects GFP-Plk5 (blue arrows) and it was selected for further studies in this work

Figure S5. Expression of Plk5 during S-phase, G2 and mitosis. A, Schematic representation of the synchronization protocol followed. B16F10 melanoma cells were synchronized in S-phase with a double thymidine block, released from the block (time=0) and treated with nocodazole 5 h. after the release. B, These cultures progress through S-phase during the first 3-4 h and arrest in

mitosis after treatment with nocodazole. C, Plk5 is detected in S-phase but gradually decreases during G2 phase (t=4 and 5 h).

Figure S6. Tissue-specific distribution of Plk5 expression at the mRNA level. A, Profile of mouse Plk5 expression obtained from microarray analysis of mRNAs at the BioGPS (http://biogps.gnf.org) using the GeneAtlas GNF1M and MOE430 datasets, showing an enrichment in cerebellum, eyes and other regions in the brain. B, Mouse Plk5 mRNA in the developing embryo. In situ hybridization using *Plk5*-specifc probes in E14.5 embryos. Arrows indicate expression enrichment in the eye, the brain cortex and the cerebellum. Data obtained from Genepaint (http://www.genepaint.org) using the 6330514A18Rik entry (Genepaint Set ID: EH3152).

Figure S7. Validation of murine and human Plk5 antibodies and shRNA. A, HEK293 cells were transfected with a vector expressing the c-myc fused murine Plk5. Different shRNAs against the the mouse Plk5 were co-transfected with the myc-Plk5 vector. An additional scramble shRNA was used (shControl). The myc-Plk5 band (about 70 kDa) detected by the Plk5-NT antibody is sensitive to the shRNA.122 (lane 2), indicating the specificity of the antibody and the effectiveness of this particular shRNA. B, In a similar experiment, HEK293 cells were transfected with a GFP-fused human PLK5 cDNA, together with different shRNAs specifically designed to silence the human PLK5 gene. The GFP-PLK5 band (about 65 kDa) detected by the human PLK5-LK antibody is sensitive to the shRNA.1272 (lane 4) and to the shRNA pool mixture (lane 5), indicating the specificity of the antibody. It is worth to mention that this antibody does not recognize the mouse myc-Plk5 protein (about 70 kDa) (lane 6).

Figure S8. Subcellular localization of mouse and human Plk5 proteins. Subcellular localization of exogenously expressed of mouse Plk5, mouse Plk5-ΔN or human PLK5 as GFP-fusion proteins in U2OS cells. The murine GFP-Plk5 fusion protein clearly labels the nuclei of Plk5-GFP positive interphase U2OS as well in HeLa, 293 and 3T3 cells (data not shown). The predicted shorter human PLK5 is however cytoplasmic and, similarly, the murine Plk5 cDNA lacking the kinase domain (N-terminus deleted; Plk5-ΔN) is also found in the cytoplasm.

Figure S9. Expression of PLK5 in different human tissues. A tissue macroarray containing 35 normal samples from human tissues was used for PLK5 immunodetection. The table describes the major cell types showing positive signal in these tissues. Representative signal is observed in tonsil, seminal vesicle, parotid gland, liver cells and in the tubules of the kidney. Most cells display cytoplasmic staining although in some cases the signal is nuclear (some cells in the tonsil). This signal is also eliminated after pre-treatment with the antigenic peptide. In other tissues, the signal is polarized in the cytoplasm (arrows in the acinar cells in the parotid gland) or restricted to specific spots within the cytoplasm (arrows in seminal vesicle and liver cells).

Figure S10. PLK5 expression in brain tumors. A, *PLK5* mRNA expression in Agilent microarrays using RNA from the brain tumor samples also analyzed by IHC. GBM: Glioblastoma multiforme (grade IV); AA: Anaplastic astrocytoma (grade III); DA: Diffuse astrocytoma (grade II);; AOA: Anaplastic oligoastrocytoma (grade III); OA: Oligoastrocytoma (grade II); AOG: Anaplastic oligodendroglioma (grade III); OG: Oligodendroglioma (grado II). These data were obtained essentially as described in (3) and show a reduction in PLK5 mRNA expression levels in advanced tumors such as GBM and AA (grade III) or AOA (grade III). B, Relative expression levels ok *PLK5* mRNA in grade II and grade III astrocytomas or comparative analysis between these astrocytomas and oligodendriomas and GBM (sourced from Oncomine). C, Lower

expression of PLK5 significantly correlates with worse survival 5 years after surgical resection and displays some correlation with 5-year survival after diagnosis. Data in B and C are collected from (4)(sourced from Oncomine). D, mRNA expression of human PLK1, PLK2, PLK3 and PLK5 in a collection of glioblastomas and oligodendrioma tumors, analized using Agilent DNA platform. PLK2 is severly downregulated in all the tumors regardless the grade level while PLK5 is only downregulated in the most aggressive glioma grades. PLK1 and PLK3 are moderately upregulated in some tumors. PLK4 was not represented in these commercial arrays. Data is normalized towards normal brain tissue expression rates. E, similar analysis as performed in D, but using a custom made DNA microarray (CNIO). In this case, only samples from 20 glioblastomas are analyzed. PLK1 and PLK3 mRNA are upregulated whereas PLK2 mRNA is downregulated. PLK4 does not show a remarkable change in expression. PLK5 was not represented in these arrays. F, mRNA expression levels of PLK family members in glioma tumors classified by malignancy grade (grade II, III and IV versus normal brain). (Data from Ref. (4) after analysis in Oncomine)

Figure S11. Induction of apoptosis after re-expression of PLK5 in glioblastoma cell lines. A172 and LN18 glioblastoma cells were transfected with GFP or the GFP-fusions of the wild-type mouse Plk5, the Plk5-ΔN mutant and human PLK5. Apoptosis was scored by Annexin-V staining and FACS analysis.

Table S1. Oligonucleotides used or the analysis of human, mouse and rat Plk5 orthologues.

Short hairpins for RNA interference		
Specificity	Code	Sequence (5'-3')
Human	sh125	GCTACAAGCTGACAGACATGT
	sh466	CTTAGTAACTTCTTCCTTAAC
	sh1272	GGTGGATTATTCCAGCAAATA
Mouse	sh122	GCTACAAGCTCACGGACAT
	sh424	CTGCGCTACTTGCACCAACAA
	sh1457	TGCGGCTCTTTGCCTGCTATA
Rat	sh122	GCTACAAGCTCACGGACAT
	sh470	CCAGTAATTTCTTCCTTAA
	sh1374	CTCCTACCAACCTGACCAA
Methylation análisis of human *PLK5*		
MS-PCR	M1-FW	AACGTCGAGGTTTATATTTTAAGC
	M1-RW	GAACTAACTAAAAACCGCTAATACG
Bisulfite sequencing	BS1-FW	TTTAGGTTTTTATGTGGGTTTTAGG
	BS1-RW	GTTTTAGGTTTTTATGTGGGTTTTAG

Supplementary References

1. **Larkin, M. A., G. Blackshields, N. P. Brown, R. Chenna, P. A. McGettigan, H. McWilliam, F. Valentin, I. M. Wallace, A. Wilm, R. Lopez, J. D. Thompson, T. J. Gibson, and D. G. Higgins.** 2007. Clustal W and Clustal X version 2.0. Bioinformatics **23:**2947-8.
2. **Rhodes, D. R., S. Kalyana-Sundaram, V. Mahavisno, R. Varambally, J. Yu, B. B. Briggs, T. R. Barrette, M. J. Anstet, C. Kincead-Beal, P. Kulkarni, S. Varambally, D. Ghosh, and A. M. Chinnaiyan.** 2007. Oncomine 3.0: genes, pathways, and networks in a collection of 18,000 cancer gene expression profiles. Neoplasia **9:**166-80.
3. **Ruano, Y., M. Mollejo, T. Ribalta, C. Fiano, F. I. Camacho, E. Gomez, A. R. de Lope, J. L. Hernandez-Moneo, P. Martinez, and B. Melendez.** 2006. Identification of novel candidate target genes in amplicons of Glioblastoma multiforme tumors detected by expression and CGH microarray profiling. Mol Cancer **5:**39.
4. **Sun, L., A. M. Hui, Q. Su, A. Vortmeyer, Y. Kotliarov, S. Pastorino, A. Passaniti, J. Menon, J. Walling, R. Bailey, M. Rosenblum, T. Mikkelsen, and H. A. Fine.** 2006. Neuronal and glioma-derived stem cell factor induces angiogenesis within the brain. Cancer Cell **9:**287-300.

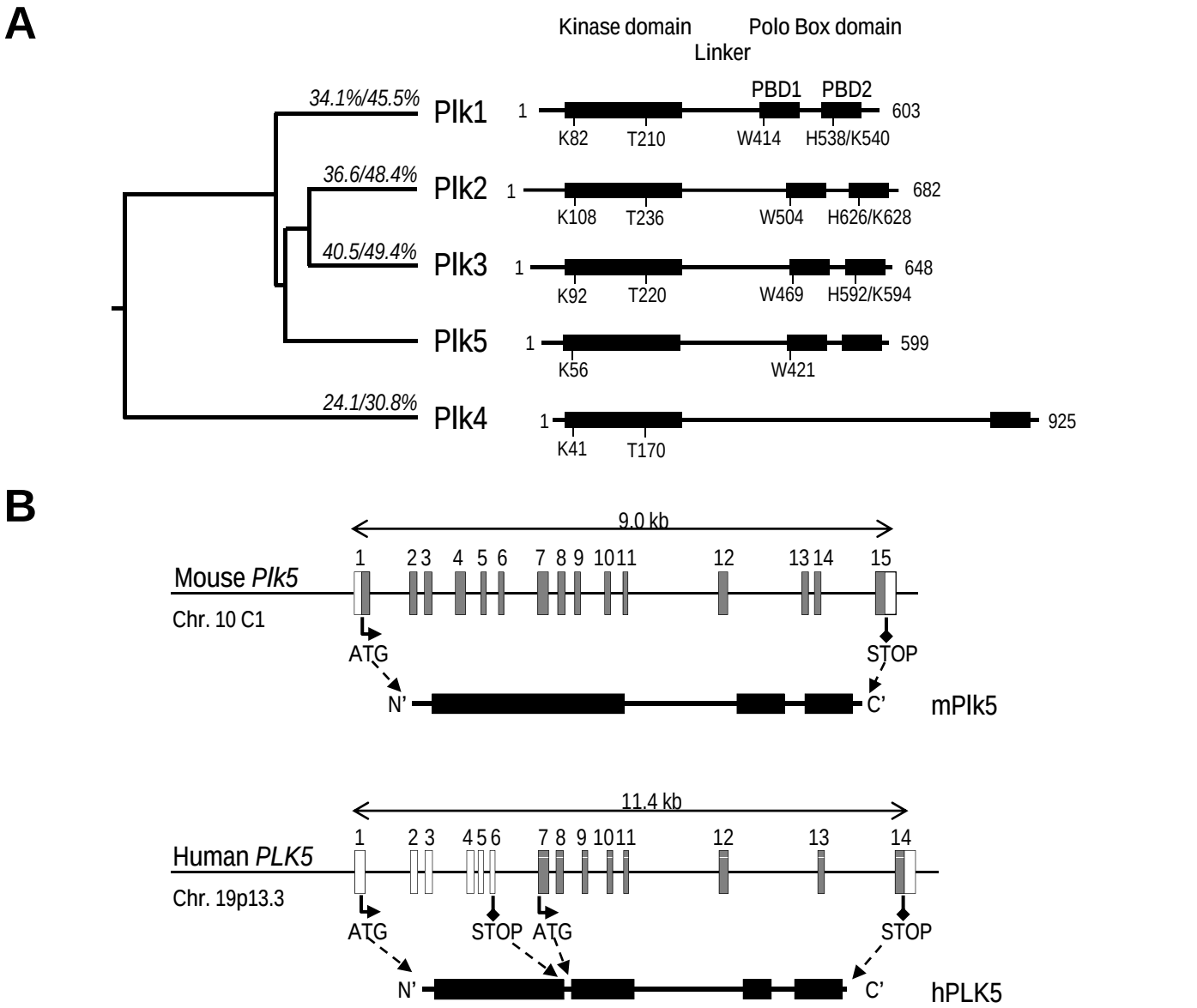
A
Kinase domain
Polo Box domain
Linker
34.1%/45.5%
Plk1
PBD1
PBD2
1
603
K82
T210
W414
H538/K540
36.6/48.4%
Plk2
682
K108
T236
W504
H626/K628
40.5/49.4%
Plk3
648
K92
T220
W469
H592/K594
Plk5
599
K56
W421
24.1/30.8%
Plk4
925
K41
T170
B
9.0 kb
Mouse Plk5
Chr. 10 C1
ATG
STOP
N'
C'
mPlk5
11.4 kb
Human PLK5
Chr. 19p13.3
hPLK5
C
ATP binding pocket
Activation loop
Plk1 188 LEVKIGDFGLATKVEYEGERKKTLCGTPNYIAPEVLSKKGHS 229
Plk2 214 MELKVGDFGLAARLEPLEHRRRTICGTPNYLSPEVLNKQGHG 255
Plk3 198 MELKVGDFGLAARLEPPEQRKKTICGTPNYVAPEVLLRQGHG 239
Plk5 166 MEVKIGDLGLAARVGPAGRCHRVLCGTPNFQAPEVVSRNGHS 207
Plk4 148 MNIKIADFGLATQLNMPHEKHYTLCGTPNYISPEIATRSAHG 189
D
PBD1
Plk1 410 WVSKWVDYSDKYGLGYQLCDNSVGVLFNDSTRLILYNDGDSLQYIERDGTESYLTVSSHPNSLMKKITLLNYFRNYMSEHL 490
Plk2 500 WVTKWVDYSNKYGFGYQLSDHTVGVLFNNGAHMSLLPDKKTVHYYAELGQCSVFPATDAPEQFISQVTVLKYFSHYMEENL 580
Plk3 465 WVSKWVDYSNKFGFGYQLSSRRVAVLFNDGTHMALSANRKTVHYNPTSTKHFSFSMGSVPRALQPQLGILRYFASYMEQHL 545
Plk5 417 WAPKWVDYSLKYGFGYQLSDGGSGVLFRDGSHMALRPQGGHVSYQPDQGTLWTFTLRDVPSPLRAKLAVLRLFACYMQRRL 497
PBD2
Plk1 511 LRTWFRTRSAIILHLSNGTVQINFFQDHTKLILCP--LMAAVTYINEK--RDFQTYRLSLLEEYGCCKELASRLRYARTMV 587
Plk2 599 LLQWLKSDKALMMLFNDGTFQVNFYHDHTKIIICNQSEEYLLTYINED--RISTTFRLTTLLMSGCSLELKNRMEYALNML 677
Plk3 565 LLQWVKTDQALLMLFSDGTVQVNFYGDHTKLILSG-WEPLLVTFVARN--RSACTYLASHLRQLGCSPDLRQRLRYALRLL 642
Plk5 516 LLSFIADSQAMVMLFSNGTVQVSLKTSQTQLVLSGEDEDLLLTLQEPGGPAVGVSYTLDVLRSHGFTLAVHHHLRHGLHLL 596

Figure S1

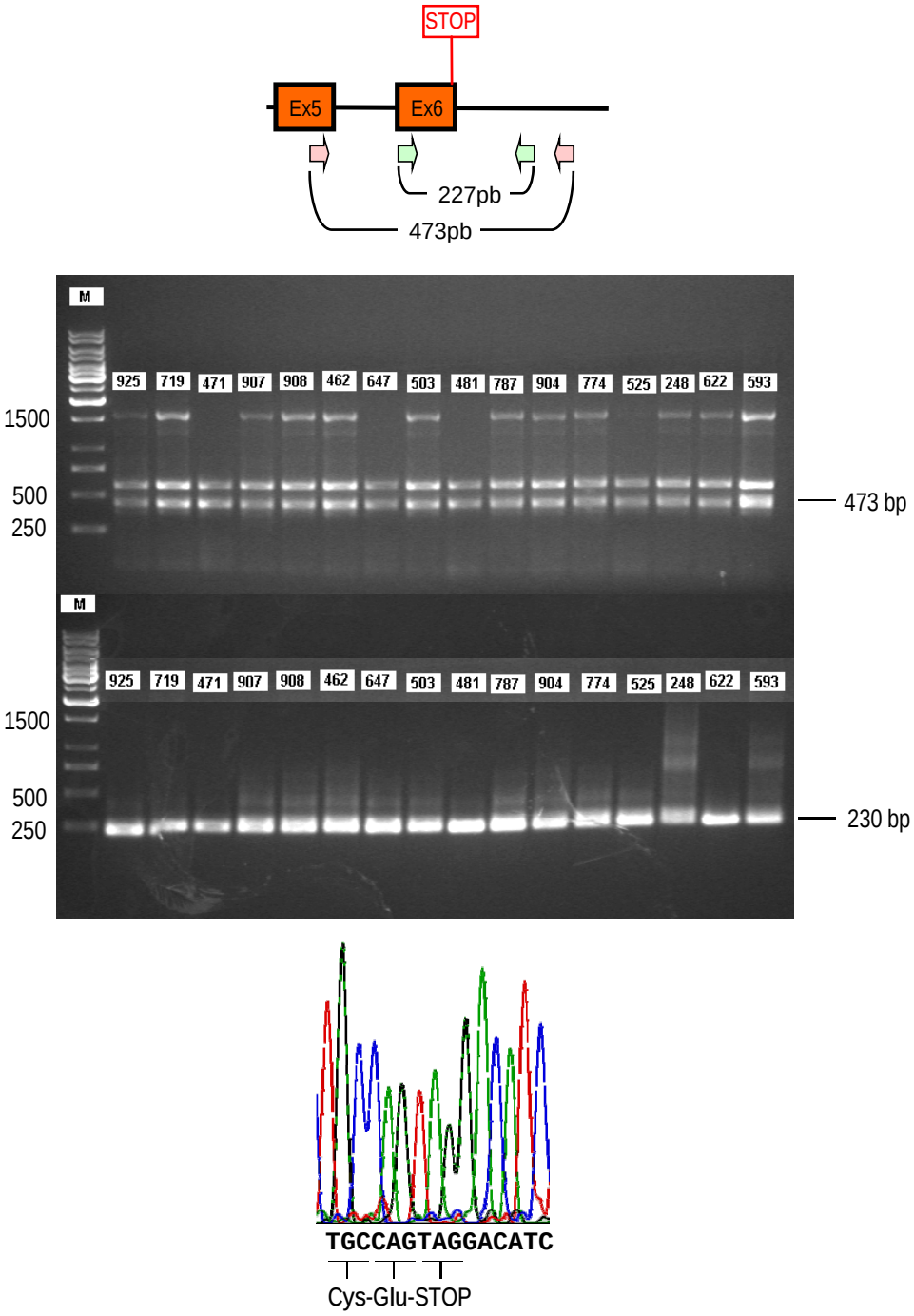
STOP
Ex5
Ex6
227pb
473pb
M
925 719 471 907 908 462 647 503 481 787 904 774 525 248 622 593
1500
500
250
473 bp
M
925 719 471 907 908 462 647 503 481 787 904 774 525 248 622 593
1500
500
250
230 bp
TGCCAGTAGGACATC
Cys-Glu-STOP

Figure S2

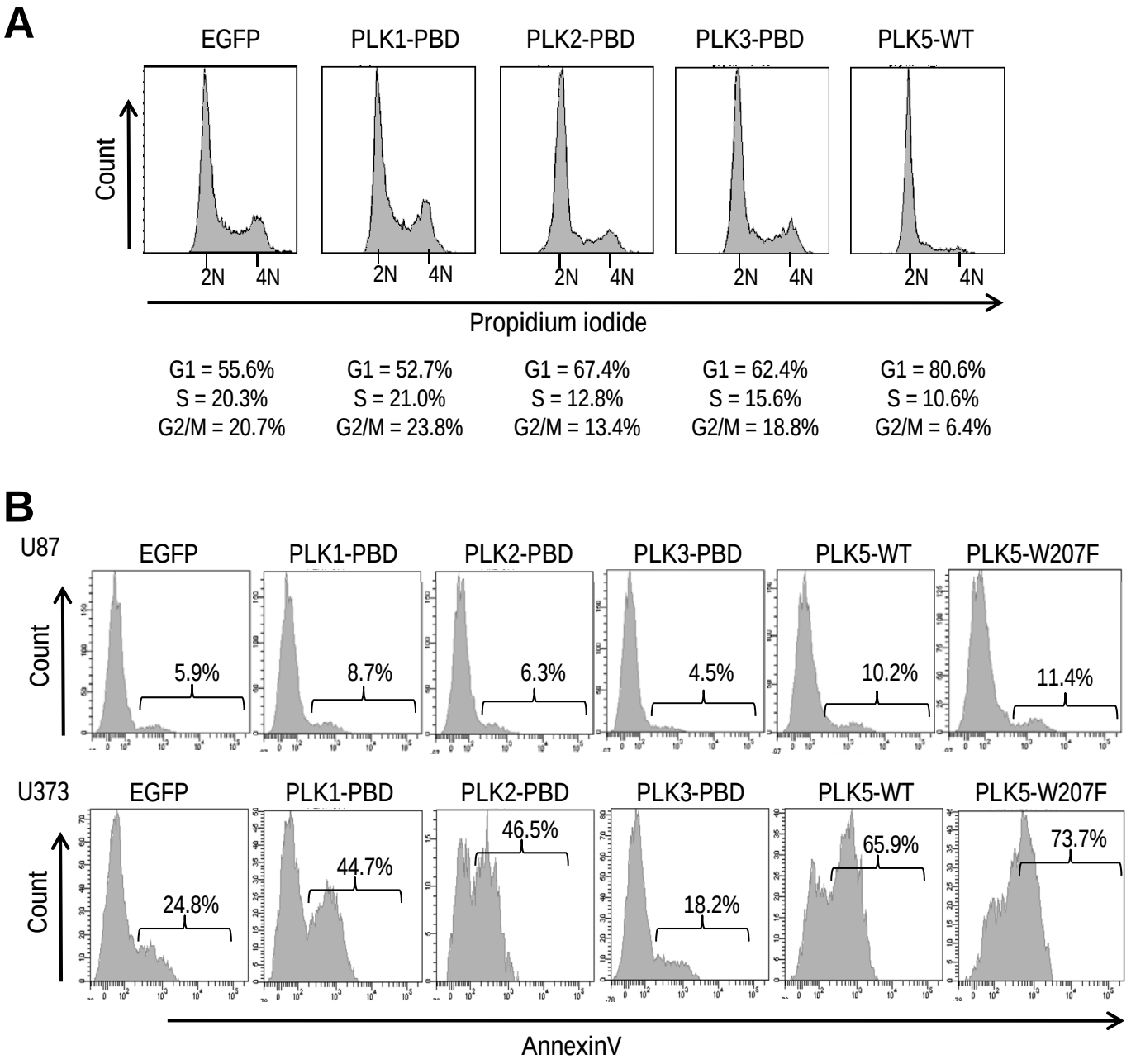
A
EGFP
PLK1-PBD
PLK2-PBD
PLK3-PBD
PLK5-WT
Count
2N
4N
Propidium iodide
G1 = 55.6%
S = 20.3%
G2/M = 20.7%
G1 = 52.7%
S = 21.0%
G2/M = 23.8%
G1 = 67.4%
S = 12.8%
G2/M = 13.4%
G1 = 62.4%
S = 15.6%
G2/M = 18.8%
G1 = 80.6%
S = 10.6%
G2/M = 6.4%
B
U87
EGFP
PLK1-PBD
PLK2-PBD
PLK3-PBD
PLK5-WT
PLK5-W207F
Count
5.9%
8.7%
6.3%
4.5%
10.2%
11.4%
U373
EGFP
PLK1-PBD
PLK2-PBD
PLK3-PBD
PLK5-WT
PLK5-W207F
Count
24.8%
44.7%
46.5%
18.2%
65.9%
73.7%
AnnexinV

Figure S3

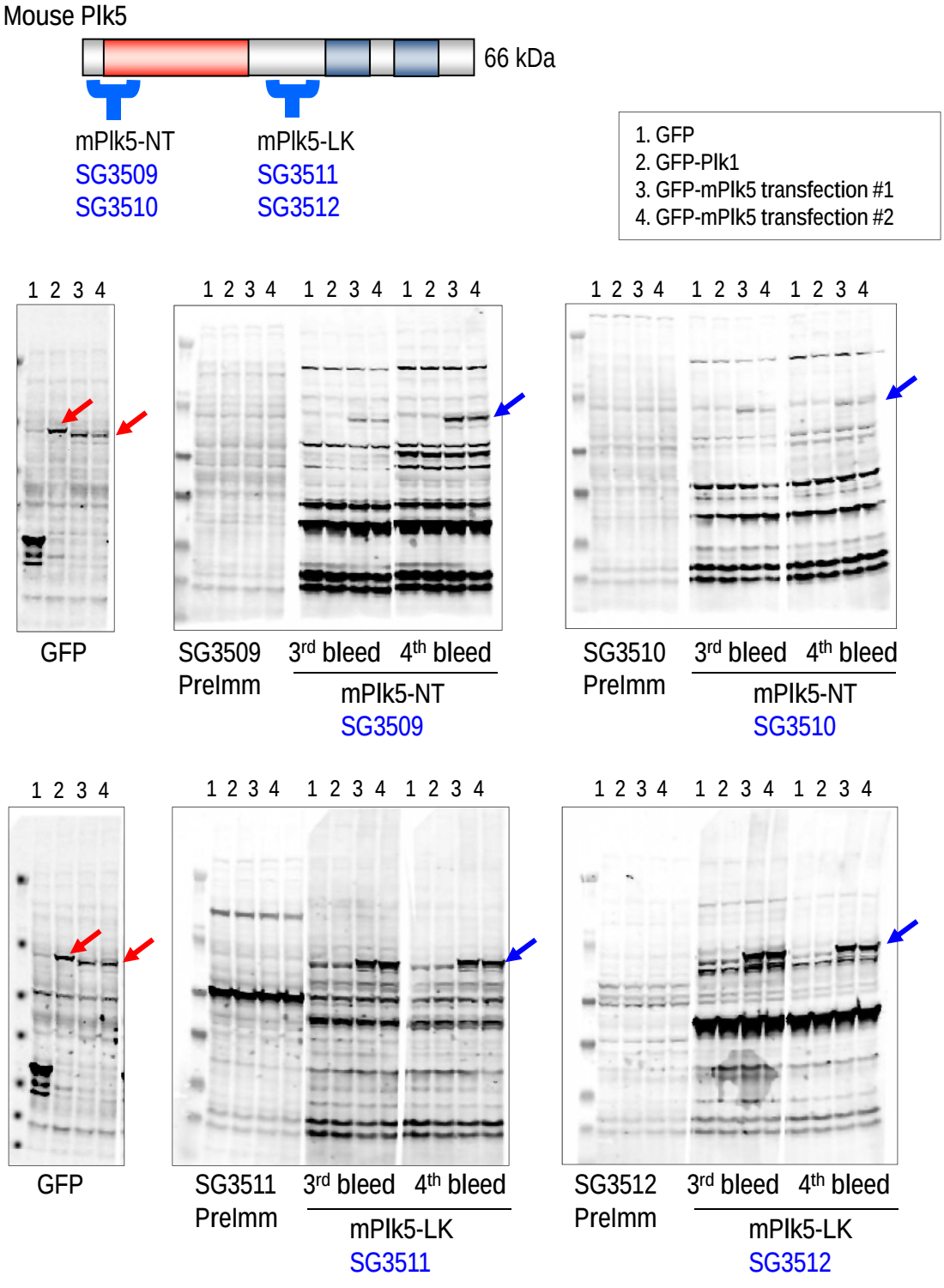
Mouse Plk5
66 kDa
mPlk5-NT
SG3509
SG3510
mPlk5-LK
SG3511
SG3512
1. GFP
2. GFP-Plk1
3. GFP-mPlk5 transfection #1
4. GFP-mPlk5 transfection #2
1 2 3 4
GFP
SG3509
PreImm
3rd bleed
4th bleed
mPlk5-NT
SG3509
SG3510
PreImm
mPlk5-NT
SG3510
SG3511
PreImm
mPlk5-LK
SG3511
SG3512
PreImm
mPlk5-LK
SG3512

Figure S4

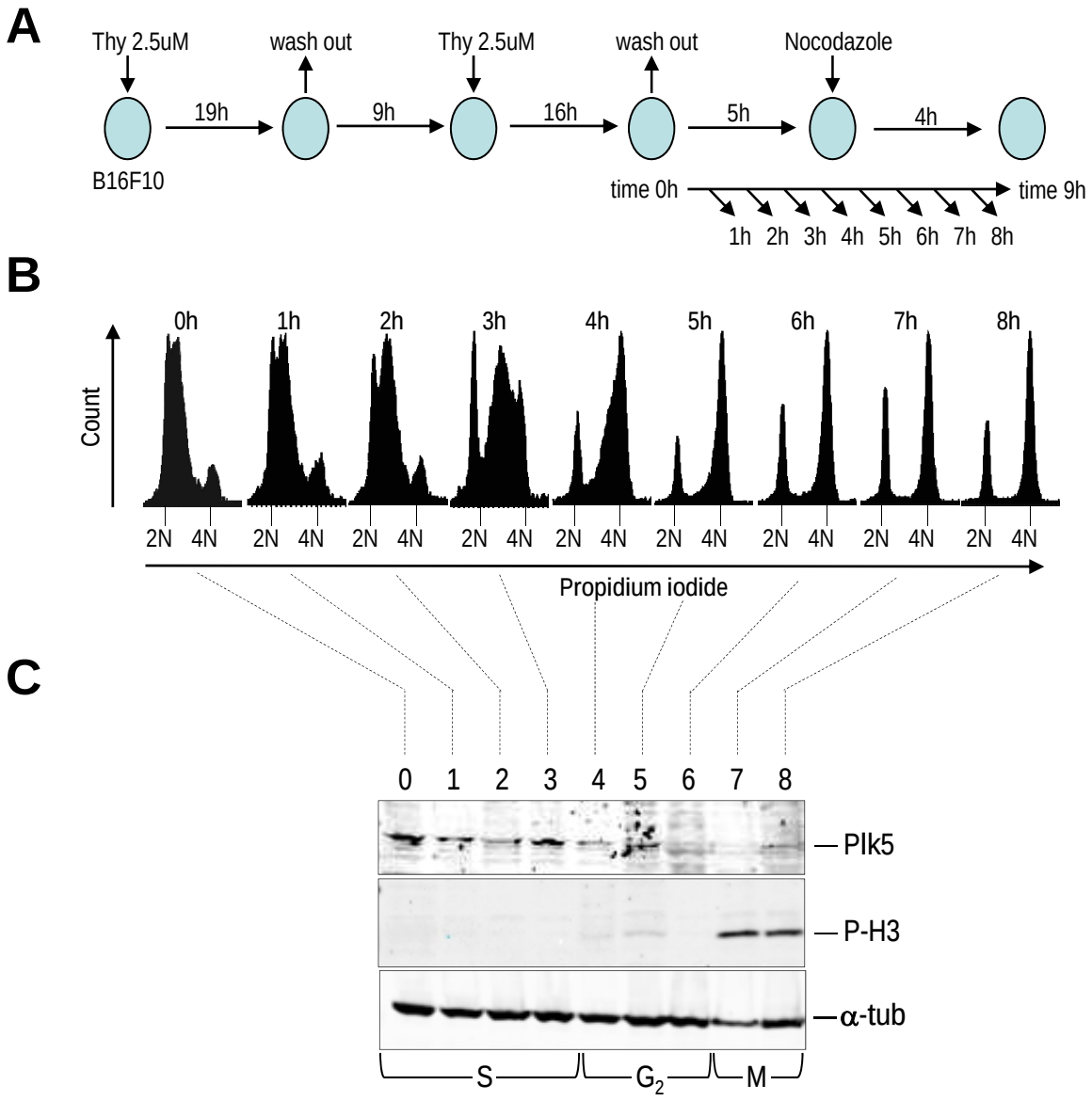
A
Thy 2.5uM
wash out
Thy 2.5uM
wash out
Nocodazole
19h
9h
16h
5h
4h
B16F10
time 0h
time 9h
1h 2h 3h 4h 5h 6h 7h 8h
B
0h 1h 2h 3h 4h 5h 6h 7h 8h
Count
2N 4N 2N 4N 2N 4N 2N 4N 2N 4N 2N 4N 2N 4N 2N 4N 2N 4N
Propidium iodide
C
0 1 2 3 4 5 6 7 8
Plk5
P-H3
α-tub
S
G2
M

Figure S5

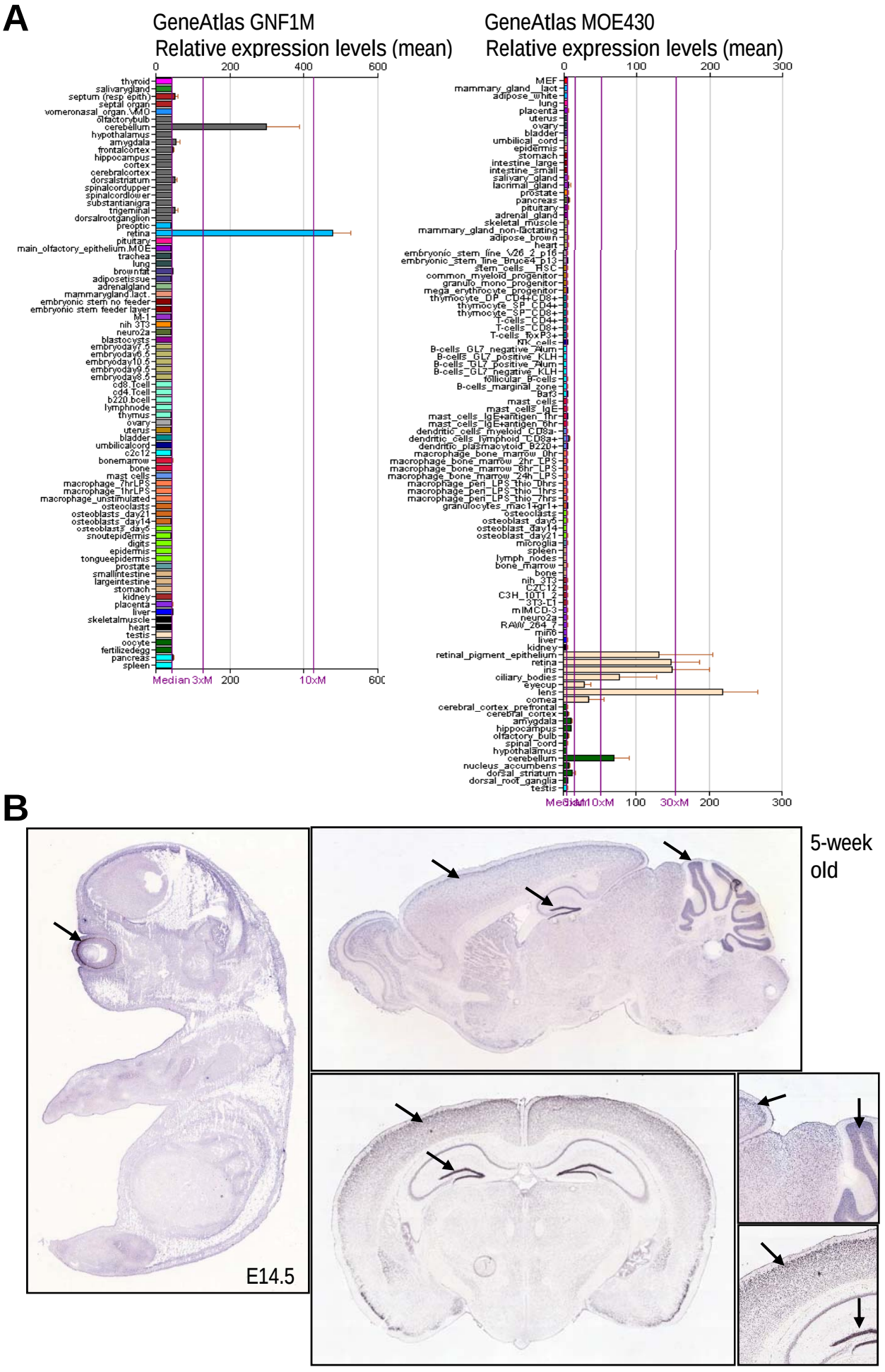
A
GeneAtlas GNF1M
Relative expression levels (mean)
GeneAtlas MOE430
Relative expression levels (mean)
B
E14.5
5-week old

Figure S6

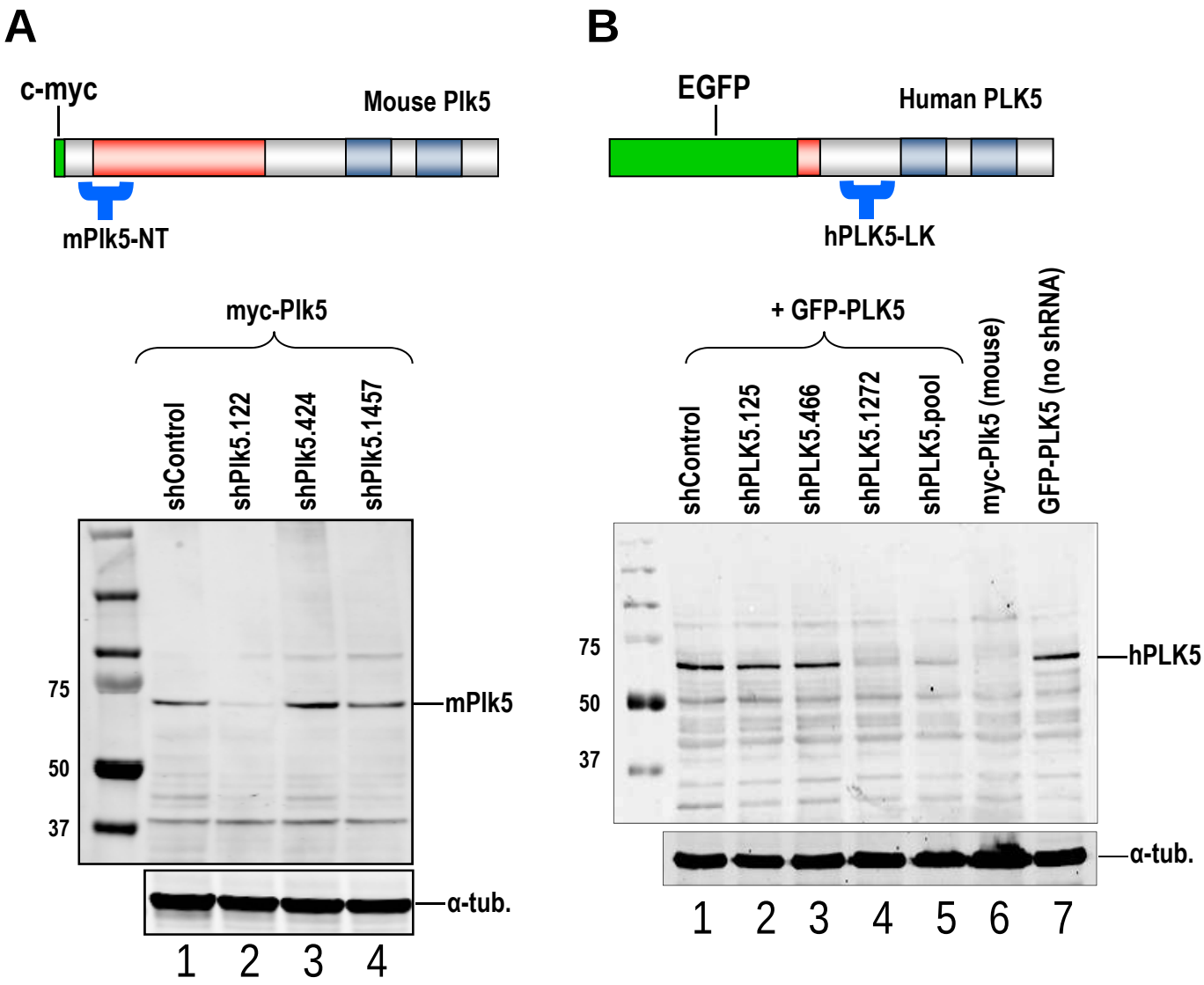
A
c-myc
Mouse Plk5
mPlk5-NT
myc-Plk5
shControl
shPlk5.122
shPlk5.424
shPlk5.1457
75
50
37
mPlk5
α-tub.
1 2 3 4
B
EGFP
Human PLK5
hPLK5-LK
+ GFP-PLK5
shControl
shPLK5.125
shPLK5.466
shPLK5.1272
shPLK5.pool
myc-Plk5 (mouse)
GFP-PLK5 (no shRNA)
75
50
37
hPLK5
α-tub.
1 2 3 4 5 6 7

Figure S7

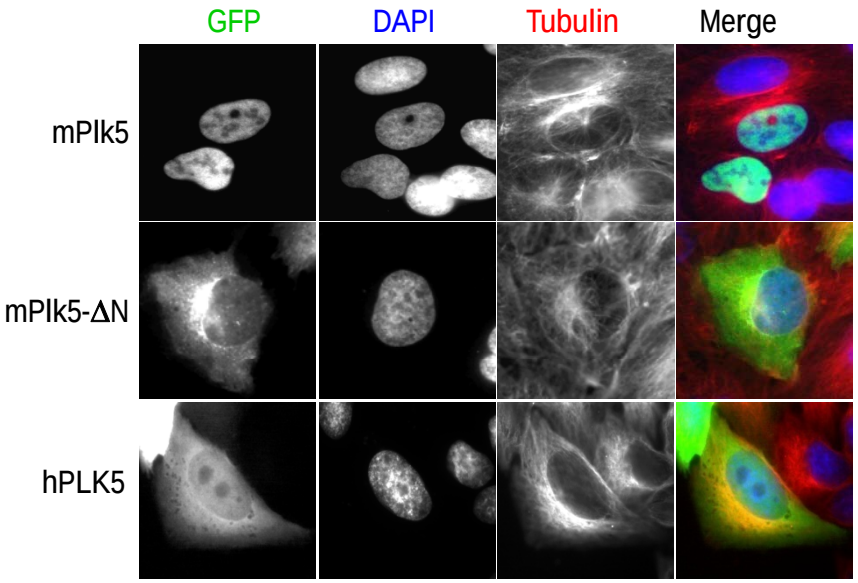

Figure S8

1. Bone Marrow	2. Prostate	3. Stomach Secretory cells ++	4. Pancreas Islets + Acines ++
5. Amygdale 1 Plasmatic cells +++ Histiocytes +; Lymph +(?)	6. Connective tissue	7. Colon	8. Liver Kufer cells + Hepatocytes +
9. Ganglion Histiocytes +	10. Seminal Vesicle	11. Duodenum Caliciform cells +++	12. Lung Neumocytes + Macrophages +++
13. Spleen Histiocytes +	14. Placenta	15. Intestine Secretory cells +++	16. Mammary Gland Distal lobules+
17. Thymus	18.Phallopian tube	19. Gall bladder	20. Thyroid Follicular cells + Endothelium ++
21. Foetal Liver	22. Uterus 1	23. Parotid Gland Serose acini ++	24. Adipose tissue
25. Appendix Caliciform cells +++	26. Uterus 2	27. Kidney Tubules + Glomerulai -	28. Oesophagus Smooth muscle +
29. Amygdale 2	30. Smooth muscle	31. Smoot muscle	32. Brain 1 Neurons +++
33. Amygdale 3 Neutrophiles + (?)	34. Skeletal Muscle		35. Brain 2 Neurons +++

Human Tissue MacroArray

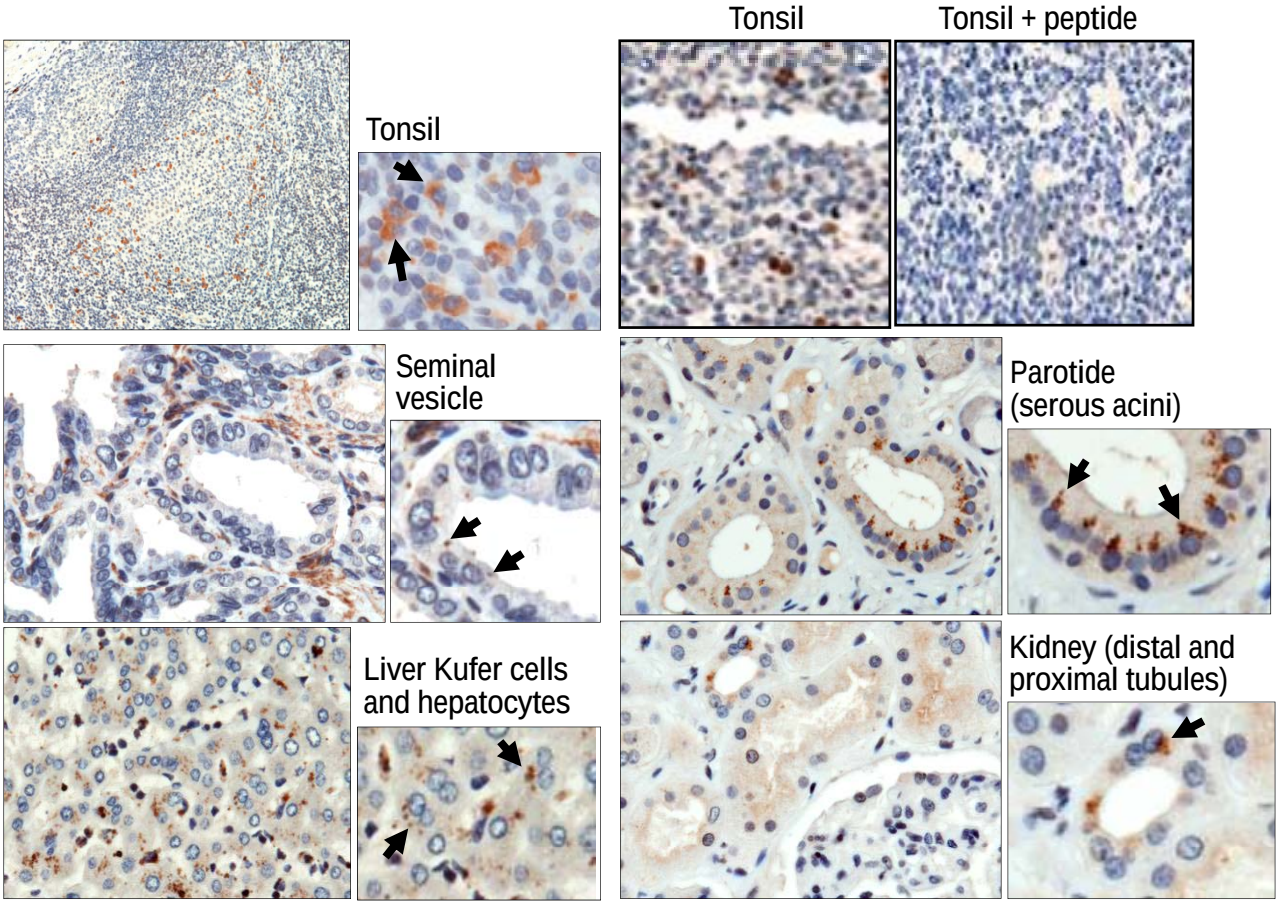

Figure S9

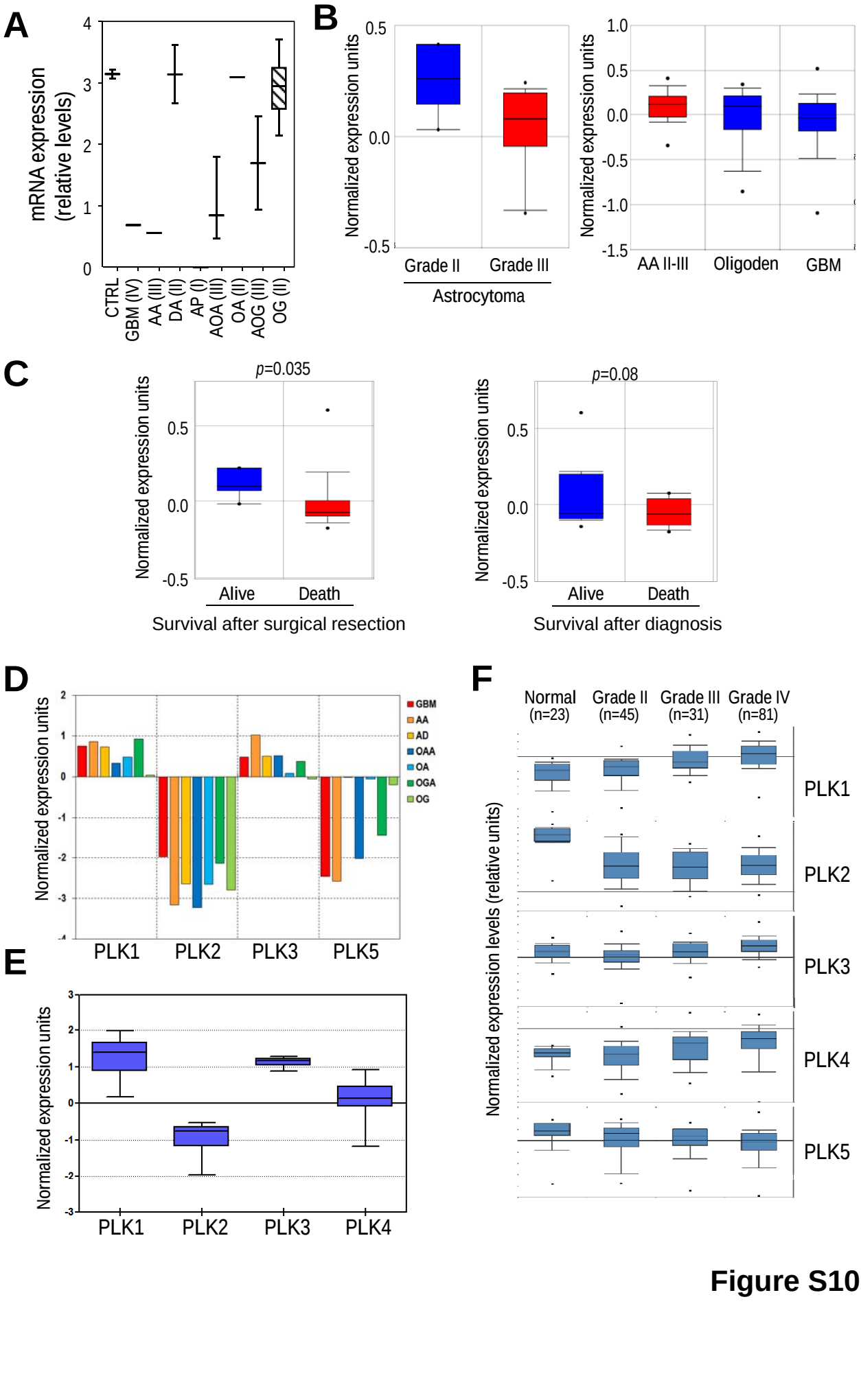
A
mRNA expression (relative levels)
CTRL
GBM (IV)
AA (III)
DA (II)
AP (I)
AOA (III)
OA (II)
AOG (III)
OG (II)
B
Normalized expression units
Grade II
Grade III
Astrocytoma
AA II-III
Oligoden
GBM
C
p=0.035
Alive
Death
Survival after surgical resection
p=0.08
Survival after diagnosis
D
GBM
AA
AD
OAA
OA
OGA
OG
PLK1
PLK2
PLK3
PLK5
E
PLK4
F
Normal (n=23)
Grade II (n=45)
Grade III (n=31)
Grade IV (n=81)
Normalized expression levels (relative units)

Figure S10

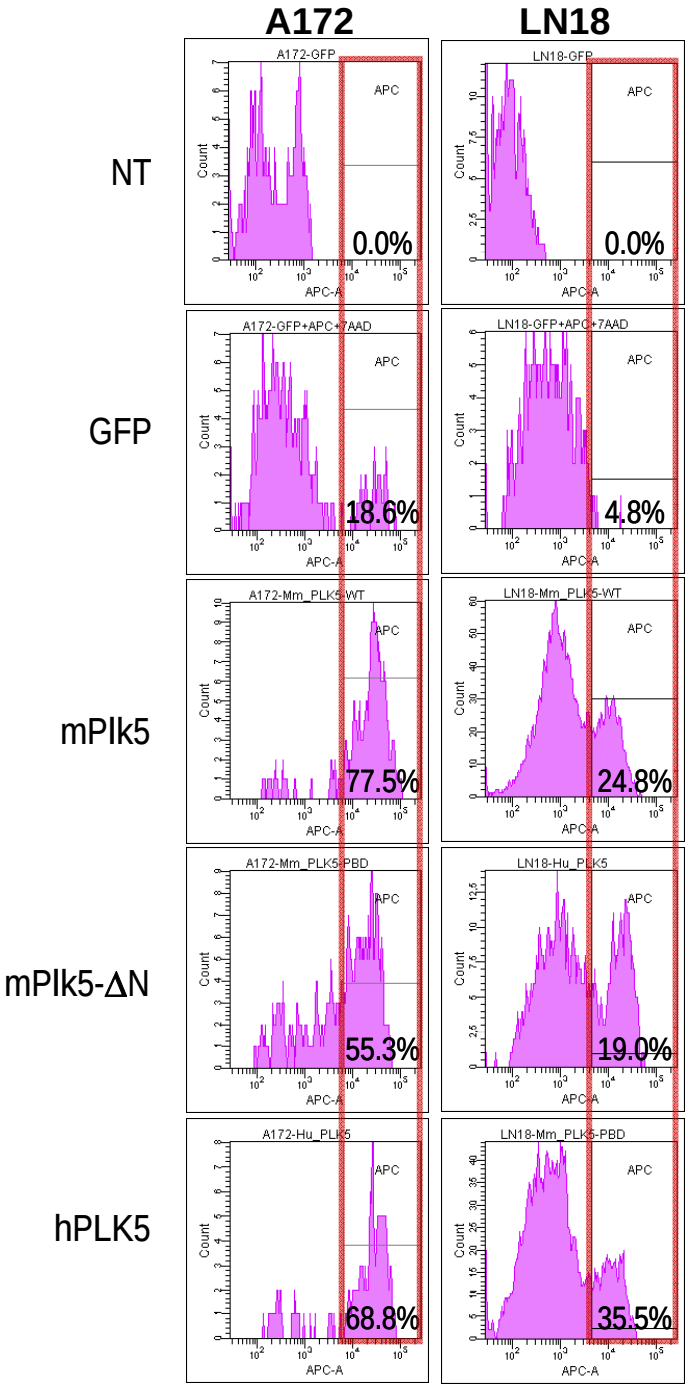
A172
LN18
NT
GFP
mPlk5
mPlk5-ΔN
hPLK5
A172-GFP
LN18-GFP
A172-GFP+APC+7AAD
LN18-GFP+APC+7AAD
A172-Mm_PLK5-WT
LN18-Mm_PLK5-WT
A172-Mm_PLK5-PBD
LN18-Hu_PLK5
A172-Hu_PLK5
LN18-Mm_PLK5-PBD
APC
Count
APC-A
0.0%
0.0%
18.6%
4.8%
77.5%
24.8%
55.3%
19.0%
68.8%
35.5%

Figure S11